

Transport barriers with shearless attractors

L. Kimi Kato and R. Egydio de Carvalho

São Paulo State University–UNESP Institute of Geosciences and Exact Sciences, IGCE, Avenue 24A 1515, Bela Vista, Rio Claro SP, Brazil

(Received 27 January 2019; published 25 March 2019)

We present a mechanism to generate a sequence of shearless curves or attractors to form a band of transport barriers. We consider the labyrinthic nontwist standard map to prepare a scenario with three shearless curves. Dissipation is introduced and three shearless attractors coexist, very close to each other. In both cases a collective transport barrier is formed.

DOI: [10.1103/PhysRevE.99.032218](https://doi.org/10.1103/PhysRevE.99.032218)**I. INTRODUCTION**

Complete transport barriers, in nonlinear systems, are spanning curves that prevent particle trajectories from entering certain regions and keep them isolated from each other [1,2]. They appear on the Poincaré map due to the persistence of invariant tori under the effect of generic perturbations. A special transport barrier is the shearless curve, named first in [3], which appears broadly in works on plasma confinement [4–9], nonlinear systems [10–22], and flow dynamics [23,24]. A global condition to the appearance of shearless tori is the presence of frequency degeneracy in the system, if it is a flow governed by a Hamiltonian, or the violation of the twist condition if it is a discrete system governed by a map [3]. Such systems present intrinsically resonances of the same order, called isochronous resonances [25]. A nontwist map has as many isochronous resonances as the order of the nontwist term. A quadratic nontwist map presents a pair of isochronous resonances. If the resonances are close enough, they can interact through the overlap of their manifolds and form a new topological rearrangement with meandering tori, among which the shearless curves can arise. The characterization of the shearless torus occurs by evaluating the winding number of the system. A remarkable feature of the shearless curve is that, in addition to surviving generic perturbations for longer periods of time, it also survives the effects of dissipation and becomes a robust attractor. In [26] it was named the shearless attractor due to its origin on the shearless torus. The system we are going to consider in the current paper is governed by a two-dimensional nontwist map previously introduced in [27] in a conservative fashion and also in [26] in a dissipative scenario. The main idea is to create a region with several nearby shearless curves or various nearby attractors in order to produce a stronger collective transport barrier. The paper is organized as follows. In Sec. II we present the model. In Sec. III the results are shown and discussed. The concluding remarks are presented in Sec. IV.

II. THE MODEL

We consider the nonlinear nontwist map called the labyrinthic nontwist standard map, introduced in [27], given

by the equations

$$\begin{aligned} y_{n+1} &= (1 - \gamma) y_n - b [\sin(2\pi x_n) + \sin(\eta 2\pi x_n)], \\ x_{n+1} &= x_n - a (y_{n+1} - r_1)(y_{n+1} - r_2). \end{aligned} \quad (1)$$

The parameter γ is responsible for introducing dissipation in the system; for $\gamma = 0$ the system is conservative. Parameter b controls the amplitude of the nonlinearity while parameter a controls the influence of the nontwist term; both affect the width of the chaotic sea. r_1 and r_2 are the positions where the resonances will be born in the phase space (x, y) , and η is the parameter that induces bifurcations inside the resonance islands. The x variable of the map has period 1. The quadratic term involving r_1 and r_2 leads to the appearance of two isochronous resonances [25] which can overlap, depending on the distance $|r_1 - r_2|$. When $\eta > 1$, bifurcations inside the islands generate new separatrices which can overlap as well. Isochronous resonances have the same period and correspond to degeneracy in frequencies. In this nontwist scenario a shearless curve can appear, which is a remarkable robust transport barrier because it has a winding number close to the golden number, the most irrational number, and thus withstands the effect of generic perturbations for longer periods of time. This point is very relevant for plasma confinement in tokamaks. Depending on the value of η it is possible to have the coexistence of more than one shearless curve, and our conjecture is that many shearless curves may produce the best scenario to obtain a more robust attractor in the dissipative case. We are going to analyze this configuration.

III. RESULTS

Figures 1(a), 1(c), and 1(e) show the effect of varying the parameter b considering the set of parameters $\eta = 3$, $a = 0.1$, $r_1 = 0.2 = -r_2$, and $\gamma = 0$. In the second column we observe the corresponding winding numbers calculated through the expression

$$\omega = \lim_{n \rightarrow \infty} \frac{(x_n - x_0)}{n}, \quad (2)$$

for which we have fixed $x_0 = 0.5$ for all calculations. To perform Eq. (2), we choose a small range for the variable y , we divide it into 1000 values, and for each value we iterate the equations of the map given in Eq. (1). After a maximum

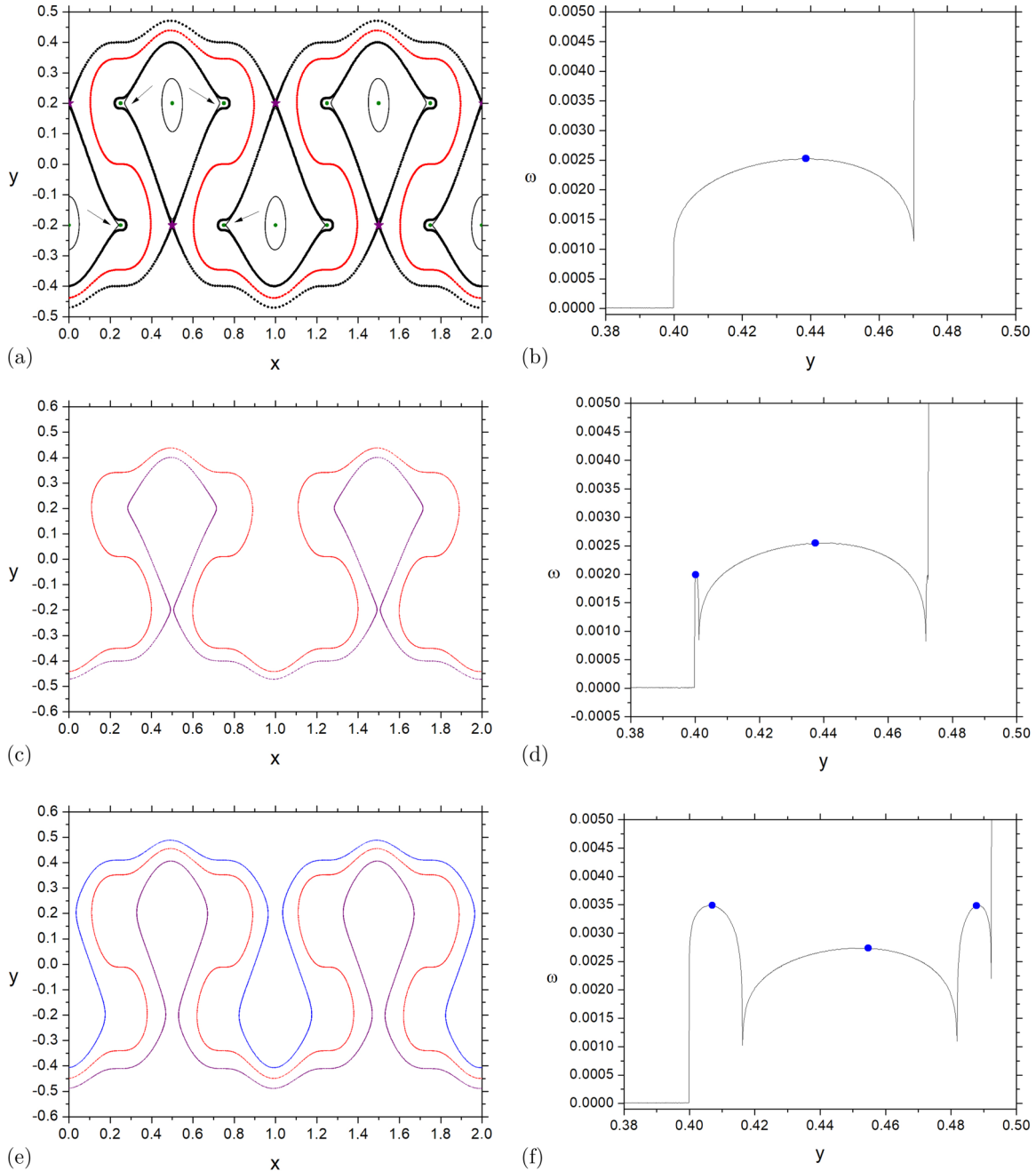


FIG. 1. The birth of shearless curves in the phase space as the parameter b is increased. In panel (a) the red curve is the only shearless curve, which is associated with an extremum in the winding number, showed in panel (b); the green dots show the elliptic fixed points, and the purple stars and black arrows show the hyperbolic fixed points. In panel (c) there are two shearless curves and in panel (d) there are two extrema, while in panel (e) there are three shearless curves and in panel (f) there are three extrema. The parameters used were $a = 0.1$, $\eta = 3$, $r_1 = 0.2$, $r_2 = -0.2$, and zero dissipation $\gamma = 0$. In panels (a) and (b) $b = 0.005$. In panels (c) and (d) $b = 0.0051$. In panels (e) and (f) $b = 0.006$.

number of iterations we take the value of x , calculate, and store the value of ω . The process is repeated for all values of y in this range. For each extremum of the winding number, i.e., $d\omega/dy = 0$, a shearless curve will appear in the phase space (x, y) .

In Fig. 1(a), we give several initial conditions in order to show more broadly the dynamics in the phase space. In the range $x : [0, 1]$ around $y \sim 0.2$, and also around $y \sim -0.2$, there are three elliptic fixed points and three hyperbolic fixed points as well. In this configuration both isochronous

resonances have already overlapped. The stable fixed points will become stable foci, i.e., point attractors, when the dissipation is introduced. The red curve is the shearless curve associated to the extremum of the corresponding winding number showed with a blue dot in Fig. 1(b). For the value $b = 0.005$, Fig. 1(a), there is only one shearless curve in the system. In Fig. 1(c) we show only the shearless curves without any other trajectory because we are interested in understanding the behavior of these curves under the effect of dissipation. Figure 1(d) shows the winding number with

two extrema marked with blue dots. In Figs. 1(c) and 1(d), we use $b = 0.0051$. Increasing the parameter to $b = 0.006$, we can observe three shearless curves in Fig. 1(e) associated with the three extrema of Fig. 1(f) also marked with blue dots. Hence, with the chosen set of parameters we prepare the system with three coexisting shearless curves, which are very close to each other in the phase space, to understand their evolution as the dissipation is increased in the system.

The dissipation is now introduced for very small values of γ in order to observe the transitions that usually occur in tiny scales. In [26], it was showed that the shearless curve becomes an attractor when dissipation is present and this attractor carries the robustness of its conservative ancestor. Based on that, and considering that in the system there are three shearless attractors, we asked how would be the possible behavior of these attractors as the dissipation is increased. We adjust the parameters to observe smooth changes in the structures of the attractors. To be successful, the dissipation should be very small because the winding number is no longer defined. However, to identify now the shearless attractors we take their coordinates of the conservative case and evolve

them for a great number of iterations and we disregard the transients of 90% of the iterations. The remaining points are attracted toward the attractors. We plot them in Fig. 2, where we keep fixed the parameters that could introduce chaos in the system in order to observe the underlying structures that support the final configuration of the shearless attractor. We fix $a = 0.1$ and $b = 0.006$ and we select four values for the dissipation parameter, $\gamma = [1; 2; 3; 5] \times 10^{-4}$.

In all the panels of Fig. 2 we did not plot the other point attractors, which exist in the system, in order to keep the focus only on the shearless attractors. We also did not plot any transients of the trajectories. We can observe in Fig. 2(a) that the three shearless attractors are closer but relatively distant in relation to the next plots. In Fig. 2(b) the outer attractors move toward the central one. The vertical straight lines are useful for guiding the eyes to observe that movement. In Fig. 2(c), we observe the same motion, and in Fig. 2(d) the three shearless attractors are collapsed into only one attractor. The interesting point here is to consider the inverse process: From one attractor can be born three attractors. It seems intuitive to us that to block transport three barriers are better than one. For the range of values used for γ we can also observe a

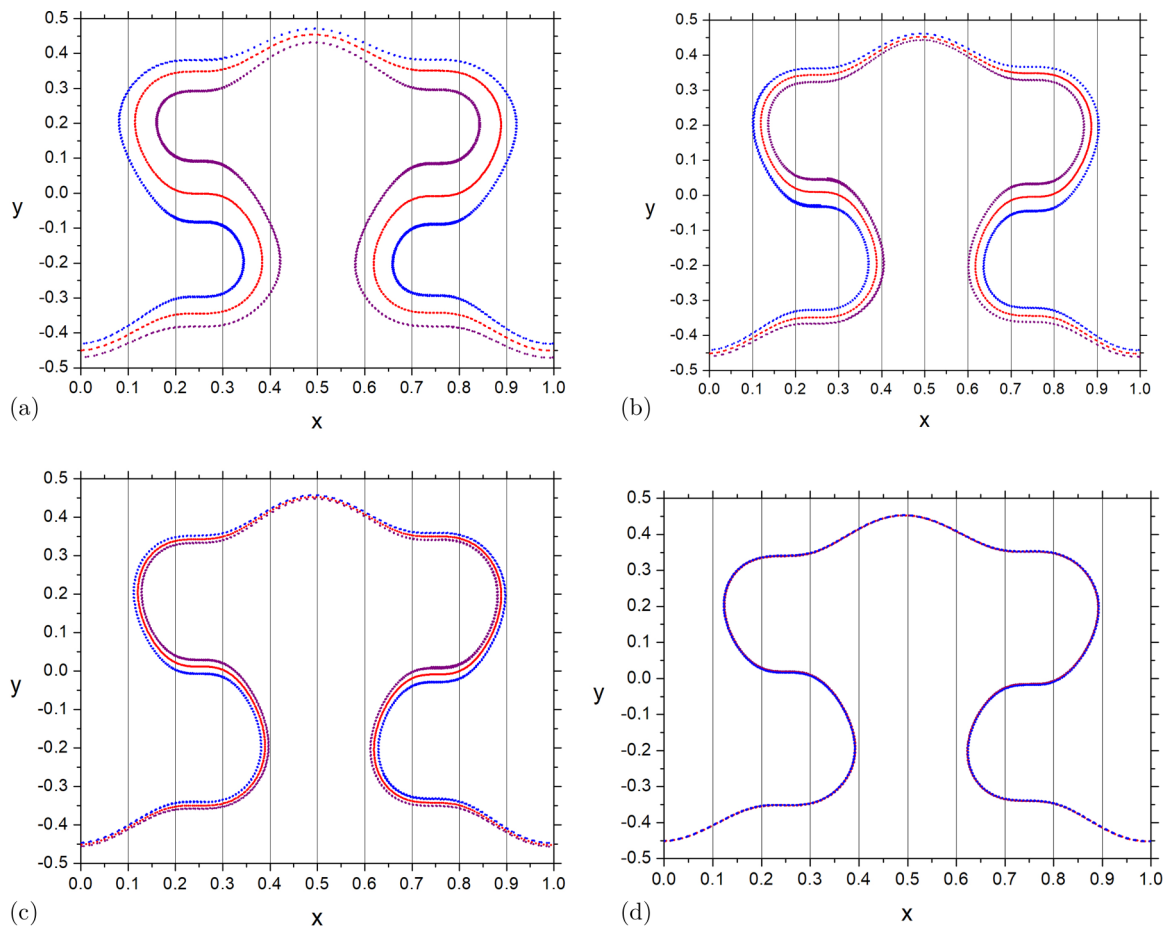


FIG. 2. Weak dissipation is introduced. In panel (a) $\gamma = 1 \times 10^{-4}$ and the three shearless attractors are smoothly deformed in relation to the plot of Fig. 1(e). In panel (b) $\gamma = 2 \times 10^{-4}$ and the central attractor is attracting the other two. In panel (c) $\gamma = 3 \times 10^{-4}$ and the formation of a single attractor is accentuated. In panel (d) $\gamma = 5 \times 10^{-4}$ and the shearless attractors collapse into only one attractor. The vertical lines are to guide the eyes.

scenario of multistability in which there is a coexistence of various shearless attractors.

IV. CONCLUDING REMARKS

We study a system that carries intrinsically the existence of shearless curves, and we propose a mechanism to form a region of robust attractors. Our model allows us to have as many shearless curves as desired, and it is well known that these curves are transport barriers that survive intense generic perturbations. They play a very important role for the plasma confinement in tokamaks, and the longer they survive the more efficient is the confinement. We change the control parameter b to evidence the birth of one, two, and three shearless curves. We prepare the system with three shearless curves and introduce dissipation transforming them into three shearless attractors, by varying the dissipation parameter γ . We observe that they collapse into only one final attractor. This is a significant mechanism to form an attractor. In fast or turbulent processes this configuration may go unnoticed, but if these processes are controlled by parameters then they can be adjusted to improve the transport barriers. This improvement will occur by considering the inverse mechanism and breaking the attractor degeneracy to form a sequence of shearless attractors. Even in the conservative scenario it is

possible to create a region with several shearless curves close to each other and produce a wider region of transport barriers. The region composed of many shearless attractors is supposed to be more robust to block transport in the system. However, to verify this point, it is necessary to have at least one free parameter other than b , since it changes the winding number profile—just as does the parameter a —and consequently changes the number of shearless curves in the system. It should also be distinct from the parameter γ , since it transforms the scenario from one attractor to three attractors. However, to verify this point, it is necessary to have at least one free parameter other than b , since it changes the winding number profile—just as does the parameter a —and consequently changes the number of shearless curves in the system. It should also be distinct from the parameter γ , since it transforms the scenario from one attractor to three attractors. This point will be the subject of further work.

ACKNOWLEDGMENTS

We acknowledge support from the Brazilian scientific agency CAPES—Coordination for the Improvement of Higher Education Personnel. R.E.C. also acknowledges CNPQ—National Council for Scientific and Technological Development Grant No. 306034/2015-8 and FAPESP—São Paulo Research Foundation.

-
- [1] A. J. Lichtenberg and M. A. Lieberman, *Regular and Stochastic Motion*, 1st ed., Applied Mathematical Sciences Vol. 38 (Springer-Verlag, New York, 1983).
 - [2] R. S. Mackay, J. D. Meiss, and I. C. Percival, *Physica D* **13**, 55 (1984).
 - [3] D. del Castillo-Negrete, J. M. Greene, and P. J. Morrison, *Physica D* **91**, 1 (1996).
 - [4] P. J. Morrison, *Phys. Plasmas* **7**, 2279 (2000).
 - [5] J. W. Connor, T. Fukuda, X. Garbet, C. Gormezano, V. Mukhovatov, and M. Wakatani, *Nucl. Fusion* **44**, R1 (2004).
 - [6] D. Constantinescu, J. H. Misguich, I. Pavlenko, and E. Petrisor, *J. Phys.: Conf. Ser.* **7**, 233 (2005).
 - [7] M. Roberto, E. C. da Silva, I. L. Caldas, and R. L. Viana, *Phys. Plasmas* **11**, 214 (2004).
 - [8] C. F. Figarella, S. Benkadda, P. Beyer, X. Garbet, and I. Voitsekhovitch, *Phys. Rev. Lett.* **90**, 015002 (2003).
 - [9] C. Hidalgo, M. A. Pedrosa, E. Sanchez, R. Balbín, A. Lopez-Fraguas, B. van Milligen, C. Silva, H. Fernandes, C. A. F. Varandas, C. Riccardi, R. Carrozza, M. Fontanesi, B. A. Carreras, and L. García, *Plasma Phys. Control. Fusion* **42**, A153 (2000).
 - [10] M. S. Santos, M. Mugnaine, J. D. Szezech, Jr., A. M. Batista, I. L. Caldas, M. S. Baptista, and R. L. Viana, *Chaos* **28**, 085717 (2018).
 - [11] K. Fuchss, A. Wurm, A. Apte, and P. J. Morrison, *Chaos* **16**, 033120 (2006).
 - [12] J. D. Szezech, Jr., I. L. Caldas, S. R. Lopes, R. L. Viana, and P. J. Morrison, *Chaos* **19**, 043108 (2009).
 - [13] C. Simó, *Regul. Chaotic Dyn.* **3**, 180 (1998).
 - [14] J. D. Szezech, Jr., I. L. Caldas, S. R. Lopes, P. J. Morrison, and R. L. Viana, *Phys. Rev. E* **86**, 036206 (2012).
 - [15] E. G. Altmann, G. Cristadoro, and D. Pazó, *Phys. Rev. E* **73**, 056201 (2006).
 - [16] E. Petrisor, *Int. J. Bifur. Chaos* **11**, 497 (2001).
 - [17] S. Shinohara and Y. Aizawa, *Prog. Theor. Phys.* **97**, 379 (1997).
 - [18] A. Apte, A. Wurm, and P. J. Morrison, *Chaos* **13**, 421 (2003).
 - [19] S. Shinohara and Y. Aizawa, *Prog. Theor. Phys.* **100**, 219 (1998).
 - [20] S. Shinohara and Y. Aizawa, *Prog. Theor. Phys. Supplement* **139**, 527 (2000).
 - [21] M. Farazmanda, D. Blazeviski, and G. Haller, *Physica D* **278–279**, 44 (2014).
 - [22] A. Wurm, A. Apte, and P. J. Morrison, *Braz. J. Phys.* **34**, 1700 (2004).
 - [23] R. P. Behringer, S. D. Meyers, and H. L. Swinney, *Phys. Fluids A* **3**, 1243 (1991).
 - [24] A. M. Manchoa, D. Small, and S. Wiggins, *Phys. Rep.* **437**, 55 (2006).
 - [25] R. Egydio de Carvalho and A. M. Ozorio de Almeida, *Phys. Lett. A* **162**, 457 (1992).
 - [26] R. Egydio de Carvalho and C. V. Abud, *Physica A* **440**, 42 (2015).
 - [27] C. G. L. Martins, R. Egydio de Carvalho, I. L. Caldas, and M. Roberto, *J. Phys. A* **44**, 045102 (2011).